Supplementary material in addition to SR-Site modeling report TR-10-11 as requested by SSM

3.1. Analysis of saturation intervals concerning long time safety during the hydration process

Ola Kristensson,

Clay Technology AB

1 Table of content

2 Introduction

The Swedish Radiation Safety Authority (SSM) points out that in (Åkesson et al. 2010), the buffer saturation process has not been directly evaluated in the light of long term safety (SSM2011-2426-81). Therefore, SSM requests an analysis where intervals in the saturation process are coupled to long time safety. SSM suggests that intervals in degree of saturation should be coupled to conditions/events that promote long term safety such as: build up of pressure to reduce microbial activity, and closure of open gaps close to the canister and deposition hole (DH) wall.

The objective of the analysis in (Åkesson et al. 2010, chapter 3) was "*Analyzing the time scale of buffer hydration"*, where buffer stands for the engineered barrier system within a DH. A number of different cases were studied by using pairs of thermo-hydraulic (TH) models. The TH-models were considered in pairs in order to somewhat account for effects of mechanics (M) without performing full THM-simulations. One of the TH-models in the pairs had properties corresponding to initial conditions and the other properties corresponding to fully homogenized conditions. This strategy was chosen in order to avoid dealing with about 15 detailed and fully coupled THM-simulations on a global scale since this type of modelling often is very challenging in terms of computational demand and numerical stability.

For enabling a structured comparison of the saturation process between models, the duration until the degree of saturation reached 99% was listed for five points in the buffer for all models. Four of the points were geometrically specified and the fifth point was the last point within the buffer reaching 99% degree of saturation. It should be noted that the fifth point may coincide with the other points.

In order to meet the request of SSM, providing an analysis where intervals in the saturation process are coupled to long time safety, local 1D axisymmetrical THM simulations are utilized to translate SKB's safety function criteria, expressed in pressure, into new criteria expressed in degree of saturation. These criteria are then applied on the global TH-models in order to evaluate the fulfillment of the safety functions.

The notes start with identifying relevant safety functions and their criteria as defined by SKB, and thereafter the strategy used to accomplish the analysis is outlined. Next, the processes coupled to homogenization, which occurs in the local models, are discussed and this is followed by describing how the new criteria were developed and refined. After this, the new criteria are applied to two cases considered in (Åkesson et al. 2010, chapter 3), and the safety function fulfillment is discussed. Finally a summary of and conclusions drawn from the analysis are given.

3 Safety functions and corresponding criteria

Conditions/events that promote long time safety as suggested by SSM (build up of pressure to reduce microbial activity, closure of open gaps close to the canister and DH-wall) are related to the so called safety functions, safety function indicators, and safety function indicator criteria for the buffer as described in the SR-Site main report. The *Safety functions for the initial temperate period after closure*, their indicators, and indicator criteria for the buffer are, (SKB 2011, Figure 8-2 and chapter 10.3.16):

Buff1. Limit advective transport
- i. Hydraulic conductivity < 10^{-12} m/s
- ii. Pressure > 1 MPa

Buff2. Reduce microbial activity
Density; high

Buff3. Damp rock shear movements
Density < 2050 kg/m^3

Buff4. Resist transformations (requirement on temperature)
Temperature < 100 °C

Buff5. Prevent canister sinking
Pressure > 0.2 MPa

Buff6. Limit pressure on canister and rock
- i. Pressure < 15 MPa
- ii. Temperature > -4 °C

When it comes to Buff2, the criterion of a "high enough density", as specified in the SR-Site main report, has here to be expressed numerically in order to be able to be evaluated. So here, a criterion where density > 1800 kg/m^3, as specified in "Buffer and backfill process report for the safety assessment SR-Can" (SKB, 2006), will be used. It should be noted that this is not what is specified in (SKB, 2011) and that there, it is pointed out that this type of criteria might not be a "true" indicator for the safety function.

The safety functions given above assume fully water saturated conditions, as stated in the SR-Site main report (SKB 2011, chapter 10.3.8):

> "*The safety functions for the buffer and backfill assumes a fully water saturated state. This should mean that the buffer and backfill need to be saturated to perform properly. However, no performance is needed from the buffer as long as the deposition hole is unsaturated, since no mass-transfer between the canister and the groundwater in the rock can take place in the unsaturated stage. The water saturation process itself has therefore no direct impact on the safety functions of the buffer and backfill.*"

Thus, with this in mind, analyzing the saturation process in the light of safety functions as defined by SKB might not be very meaningful. According to SKB's definitions it is only the final state of the saturation process, the saturated state, that matters for safety and for which the safety function indicator criteria have been designed.

It should, however, be mentioned that the condition of microbes at unsaturated states has not yet been scrutinized in detail. There is an ongoing project ("Gradientförsök") which addresses this issue, but no conditions are yet available, so currently an evaluation regarding this is not possible. Thus, dependent of the outcome of the ongoing microbe-project, safety function Buff2 might not only assume fully water saturated conditions, and might be extended with additional criteria.

Going back to what is given at the time when these notes are written, and studying the safety functions and theirs criteria, it can be seen that all but Buff4 (only given as a temperature criterion) are connected to restrictions on pressure (p) or density (ρ) at full saturation,

Buff1. Limit advective transport
$p > 1$ MPa
Buff2. Reduce microbial activity
$\rho > 1800$ kg/ m^3
Buff3. Damp rock shear movements
$\rho < 2050$ kg/m^3
Buff5. Prevent canister sinking
$p > 0.2$ MPa
Buff6. Limit pressure on canister and rock
$p < 15$ MPa

, respectively.

Among the criteria, the upper limits on pressure and density, given by Buff3 and Buff6, are more or less avoided by a suitable choice of initial state of the EBS and these are therefore not analyzed here.

The lower limits could be more relevant to investigate in the present context since the time when these limits are reached during the simulated saturation process may be studied. Again, however, it should be remembered that the "true" criteria as defined by SKB assume fully water saturated conditions. This is particular so for Buff5 since creep of the buffer material at unsaturated states must be considered insignificant and the criteria of this safety function will therefore not be evaluated. Thus, left to be studied are Buff1 and Buff2.

If adopting a highly simplified view on the hydro-chemo-mechanical processes in the buffer, by omitting path dependence present both in retention and mechanical behavior and also dependence on chemistry within the system, a "typical" one-to-one relation between density and pressure at full water saturation (a so called "swelling pressure curve") may be used. The lower density limit of 1800 kg/m^3 may then be expressed as being approximately equal to a limit in pressure of 2 MPa (SKB, 2006). Thus, the criteria to be investigated may be reformulated as:

Buff1: $p > 1$ MPa in order to limit advective transport

and

Buff2: $p > 2$ MPa in order to reduce microbial activity.

It is again stressed that the criterion related to Buff2 is not according to what is given in (SKB, 2011). The criterion used, obtained from (SKB, 2006), was chosen in order to have a numerical value for the analysis.

4 Strategy for the analysis

If to study when the criteria (pressures) are reached, the natural step would be to perform THMC-simulations, because pressure, within the system we look at, depends on all these processes. This is, however, out of scope of the present work, and would be a totally different task, much beyond the intention of the "original" described in (Åkesson et al. 2010, chapter 3). There, the main objective was to analyze the time scale of buffer hydration, which was performed by direct consideration of TH processes and indirect consideration of mechanical effects, i.e. pressure is not available from these models.

Therefore, in the next chapter, plane axisymmetric THM-models, similar to those described in (Åkesson et al. 2010, chapter 3.4 and chapter 5.4), will be used to develop criteria for Buff1 and Buff2 expressed in degree of liquid saturation, S_l. The new criteria, expressed in liquid degree of saturation, may then be applied on the global TH-models presented in (Åkesson et al. 2010, chapter 3). The translation from "pressure criteria" to "degree of saturation criteria" is performed by evaluating the pressure criteria in the local THM-models and then trying to find a relation to degree of liquid saturation.

If omitting chemical aspects, except what may implicitly be regarded when choosing constitutive relations and parameter values, the problem formulation necessary for studying the present issue is in line with what already has been dealt with in (Åkesson et al. 2010, chapter 3.4 and 5). There, plane and axisymmetrical THM-simulations were performed for a model representing a disc of buffer, similar to the KBS-3V design, at canister mid-height.

In this context it also seems relevant to remind about another part of the supplementary material to SR-Site requested by SSM, *Task 1.3 Description of how the "CRT-model" was used and how THM and TH models differ in terms of analyzing the hydration process*, since it relates to the studies undertaken in chapter 3.4 and 5.4 of Åkesson et al. (2010).

The global and local models used in this study and their specific features are given in Table 1 and Table 2, respectively. Detailed information about the global and local models can be found in (Åkesson et al. 2010, chapter 3.2) and (Åkesson et al. 2010, chapter 5.4), respectively.

Table 1. Global models used in this study.

Model name	Model identification	GiD-dir.
2I	Initial state model, K_R=10^{-12} m/s	THsat13.gid
2H	Totally Homogenized state model, K_R=10^{-12} m/s	THsat14.gid
8I	Initial state model, K_R=10^{-13} m/s	THsat20I2.gid
8H	Totally Homogenized state model, K_R=10^{-13} m/s	THsat20H4.gid

Table 2. Local models used in this study. Model identification by the deviation in the pellet slot material representation from that of model CRT 6b in chapter 5.4 of Åkesson et al. (2010).

Model name	Model identification	GiD-dir.
TEP_new_12	K_{min} = 1 MPa, k_{s0} = 0.1, α_i = 0	TEP_new_12.gid
TEP_new_14	K_{min} = 1 MPa, α_i = 0	TEP_new_14.gid

5 Development of new criteria expressed in S_l

The purpose of the local THM models is to provide information for the development of representative criteria for Buff1 and Buff2 expressed in degree of liquid saturation, S_l. The first step is to formulate a first version of criteria based on obtained magnitudes of degree of liquid saturation when the pressure obtain the values 1 MPa and 2 MPa. In the next step, the times until the degree of liquid saturation criteria are fulfilled in global TH models (at canister mid-height) are compared with the times for which the pressure criteria of Buff1 and Buff2 are fulfilled for the local THM models. Based on the outcome of the comparison, the degree of liquid saturation criteria are evaluated and refined.

A schematic sketch illustrating the relation between the used models in this study is shown in Figure 1. To the left of the vertical hatched line we have models on a global scale. In theory, the most general model is a THM-model (which we here do not have access to), and somewhat less general are the available pairs of TH-models with immobile mechanical representations (Initial or Homogenized) presented in (Åkesson et al. 2010, chapter 3). In the following, the pairs (2I, 2H) and (8I, 8H) will be considered. To the right of the vertical hatched line in Figure 1 the local scale THM-models are illustrated. As indicated in Figure 1, the local models will only be representative for a disc of buffer at canister mid-height, if the prescribed BCs are representative for the "global conditions" at this position.

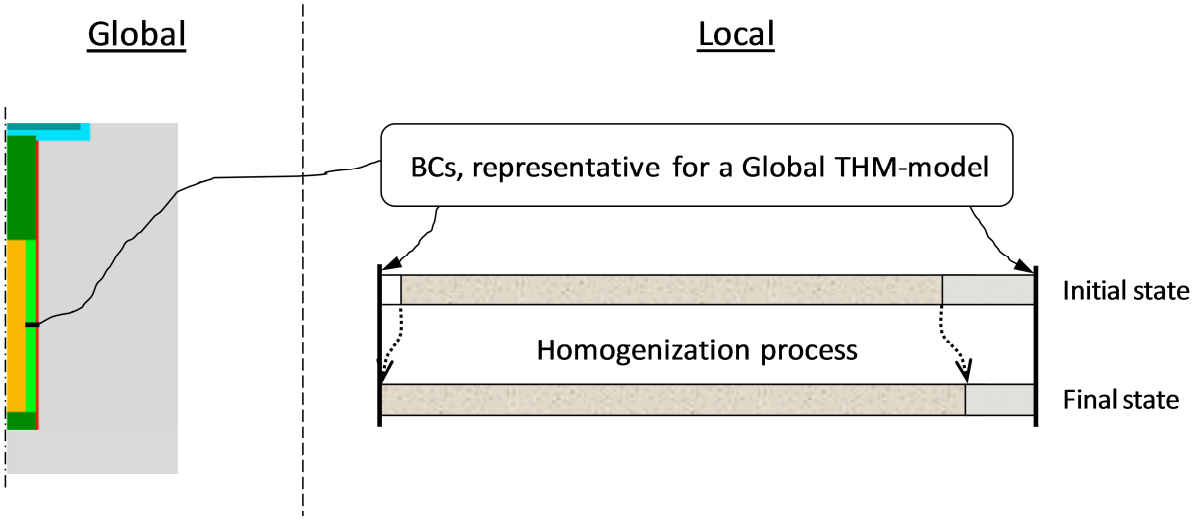

Figure 1. *Illustration of the relations between models used in this study. Global models are visualized to the left. To the right, a schematic local model geometry, to represent an axisymmetric disc at canister mid-height, is visualized. To the right of the schematic local geometry the states considered are indicated.*

The solutions of one pair of global TH-models, (2I, 2H), are utilized for designing BCs used in the local models. The global TH-models are described in detail in (Åkesson et al. 2010, chapter 3.2 and 3.3). In short, these models are considered a pair of base case models without explicit fracture representation and a lower choice of hydraulic rock conductivity ($K = 10^{-12}$ m/s). The extracted BCs at canister mid-height are: (1) radial heat flux at the canister surface, (2) temperature at the hole wall, and (3) liquid pressure at the hole wall, all three are shown in Figure 2.

As can be seen in Figure 2, the chosen conditions for the two models are quite alike. Thus, the mechanical representations of the buffer seem not to affect the TH-processes on the "outside" of the buffer to a great deal. Due to the similarities between the models' conditions, only the responses of 2H are used when designing BCs. In Figure 2, symbols indicate points between which linear interpolation was made when forming the BCs.

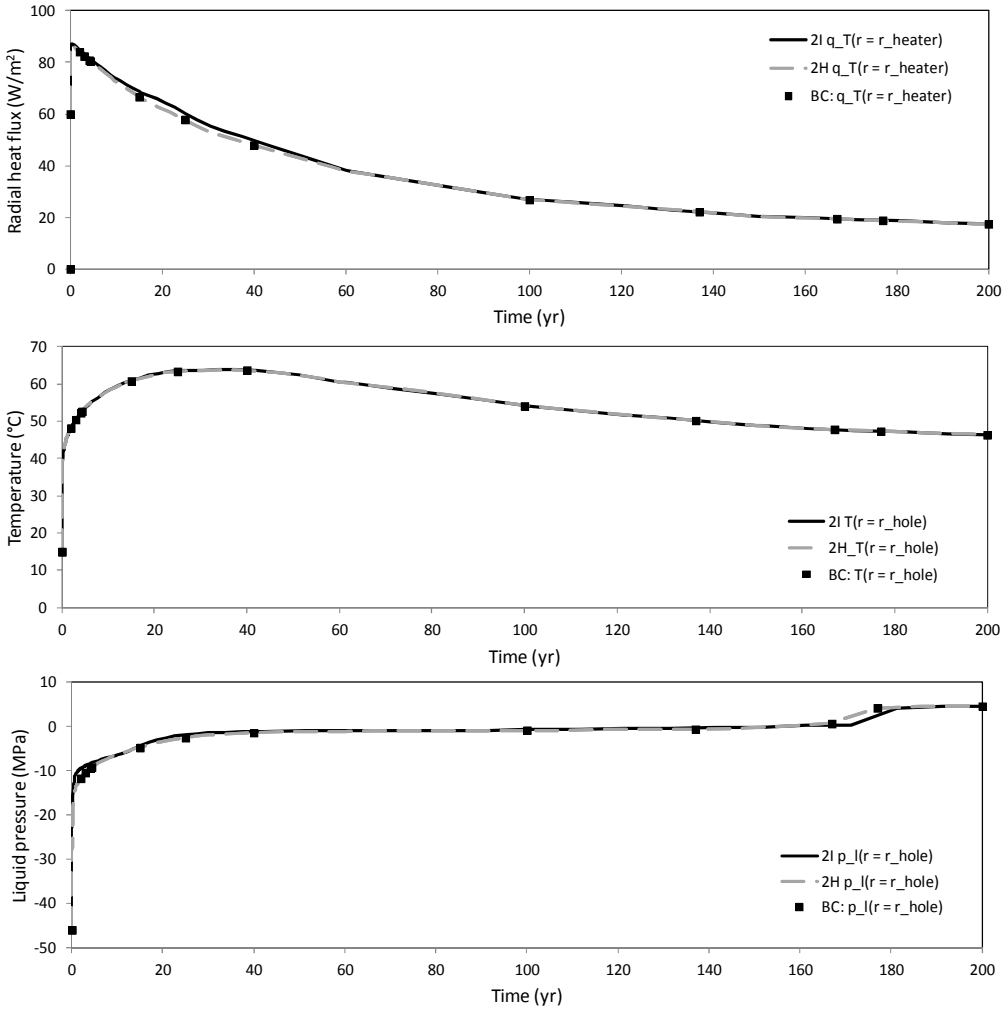

***Figure 2**. Responses for the global models and corresponding boundary conditions for local models: radial heat flux at the canister surface (top), temperature at the hole wall (mid), and liquid pressure at the hole wall (bottom).*

Model CRT_6b, described in chapter 5.4 of (Åkesson et al. 2010), was used as the starting point for the local models. In these, however, the parameters of the mechanical material model of the pellet slot material had to be altered, as compared to CRT_6b, to produce a representative porosity profile at full water saturation, relevant for slow water saturation processes. To obtain estimates of representative averaged porosities for the block and pellet slot, the graph in Figure 5-14 in (Åkesson et al. 2010), repeated below in Figure 3, was used. The graph presented in Figure 3 was produced using the analytical model described in chapter 5.3 of (Åkesson et al. 2010). The input to the analytical model was chosen as; block void ratio e^b = 0.72-0.73, pressure ratio α = 0.8-0.9, and an assumption of a "parallel wetting process", which can be considered representing a slow wetting process. The obtained output, a range in pellet slot void ratio, became e^p = 0.75-0.78. Two local realizations, as defined according to Table 2, were developed in models denoted TEP_new_12 and TEP_new_14.

Before addressing the criteria translation from pressure to degree of saturation, we take the opportunity to study the mechanical process in the models in order to visualize the homogenization process and also where and when Buff1 and Buff2 are fulfilled in the models. It could also be mentioned that a mesh dependency study was performed for model TEP_new_12 by using three times the number of elements radially in the pellet slot and block volumes in a new model (TEP_new_12_fine). No significant mesh dependency could be seen as shown in Appendix A .

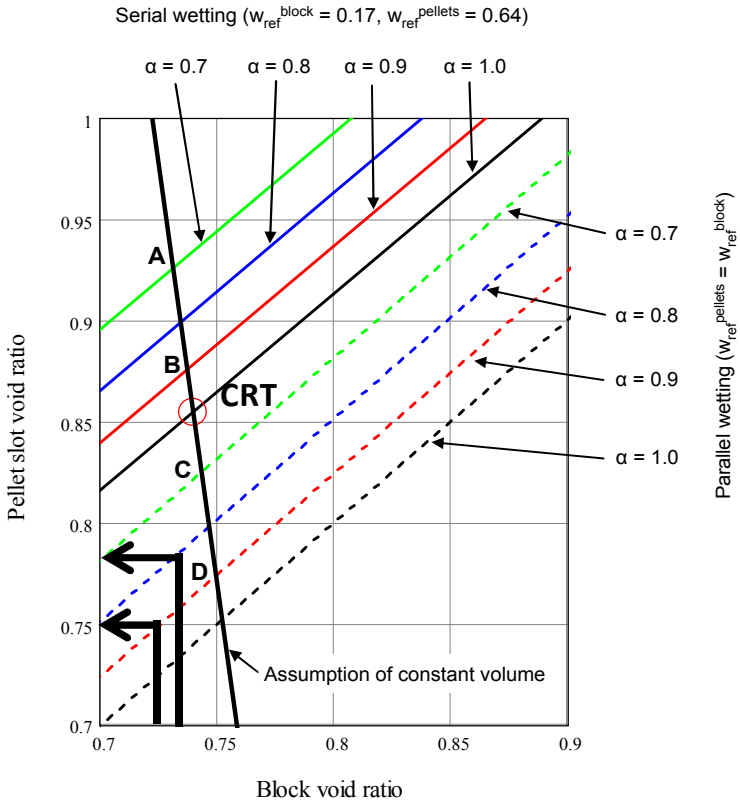

***Figure 3**. Compilation of solutions using the analytical model described in chapter 5.4 of (Åkesson et al. 2010). The black thick arrows indicate the pellet slot void ratios, e^p = 0.75 and e^p = 0.78, obtained from applying the input (e^b = 0.72, α = 0.9, parallel wetting) and (e^b = 0.73, α = 0.8, parallel wetting), respectively. This graph is a part of Figure 5-14 in (Åkesson et al. 2010).*

5.1 Local model responses

The graph at the top in Figure 4 shows void ratio profiles obtained after completed simulations together with the initial void ratio profile. Also, two arrows indicate the change in position and void ratio for two points in the TEP_new_12 model. Comparing with the initial state, the buffer has evolved into a considerably more homogenized state. The pellet slot material has been compressed by the "more strongly" swelling block material. The left arrow, showing initial and final state of a point in the block close to the initially open inner slot, indicates the swelling character in this part of the buffer. The right arrow, belonging to the pellet slot, indicates the compression taking place in this part of the buffer.

The lower part of Figure 4 is a blow-up of the final state in terms of void ratio. Beside the numerical models results, given as profiles (symbols) and volume averages (black lines),

$$\mathrm{VA}(\cdot) \equiv \frac{1}{V}\int (\cdot) dV \,,$$

over the block and pellet slot, also the analytical solutions, obtained from using the information in Figure 3, are given (grey thick lines). The pellet slot representations as described in Table 2 were chosen as to generate volume averages in close agreement with the analytical solutions, and as can be seen this is also the case.

One more check of the agreement between the analytical and numerical solutions can be performed by comparing the pressure ratio $\alpha = p_p/p_b$. In the analytical solution the pressure ratio, given by the ratio of volume averages of pressure over the pellet slot and block, was chosen as $\alpha = \{0.8, 0.9\}$. For both local models $\alpha = 0.85$ which clearly agrees well with the input to the analytical model.

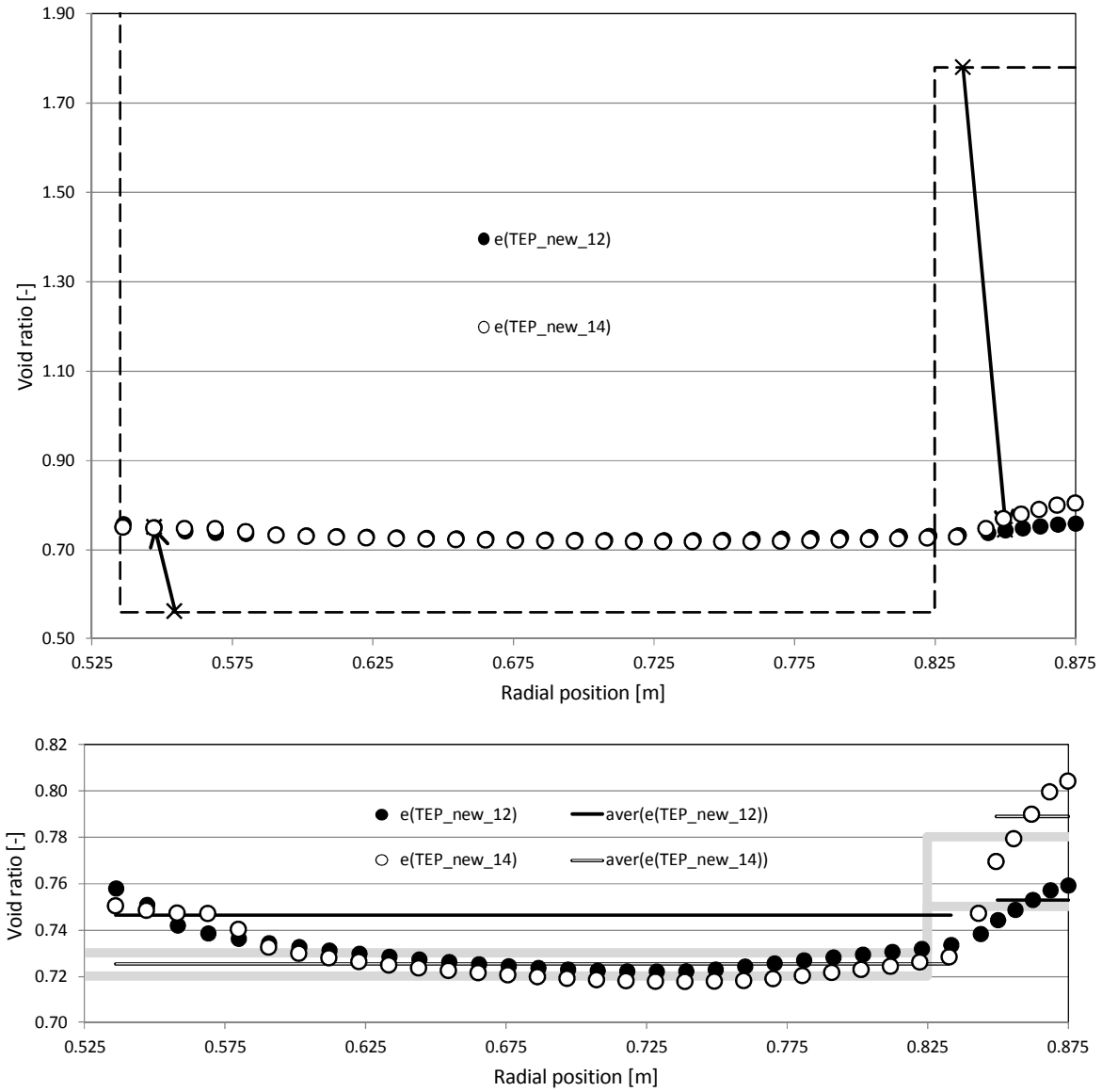

Figure 4*. Void ratio profiles obtained for the two local models at full simulation time. The initial profile (hatched line) and the two solutions (symbols) are shown at top where the arrows indicate initial and final states for two different nodes belonging to TEP_new_12. The bottom graph shows a close up at the final state for both models (symbols) with the analytical solution (grey thick line) also indicated as well as the volume averages (thin lines) over block and pellet slot for the model solutions.*

To visualize the closure of the open gap close to the canister and the homogenization process of the buffer, Figure 5 shows the path of material particles (grey lines), initially positioned with equal distances, for both local models. The interfaces (inner empty gap, block) and (block, pellet slot) are also indicated (solid black lines). An isoline consisting of (time, position)-pairs, for which the deformation is 0.99 of the final deformation is also given in Figure 5 (hatched line with symbols). Solution data are given in Table 3.

When studying the particle paths, it can be seen that the deformation of the block material can be thought of as belonging to two modes: (1) swelling into the pellet slot and (2) inner slot closure. Initially, an instant rapid compression of the pellet slot can be seen when the outer part of the block

takes up water and expands. When water reaches further in, the open inner slot begins to close and finally the block has expanded all the way to the canister. The two "deformation modes" listed above act in different directions, thereby the visible kink on the particle paths at the time when the inner slot closes.

As for the character of the final stage of deformation it can be somewhat understood by studying the appearance of the isoline. The most obvious feature is that the material close to the canister is the first to cease deforming with the extreme at the inner slot closing after 11 - 14 yr. At radii < 0.625 m there is, with increasing radius, a gradual halt of the deformation from 11 -14 yr to about 154 yr, which also is the maximum value for the entire buffer. For radii > 0.625 m the halt of the deformation is taking place "more simultaneous", in a time range about 120 – 145 yr.

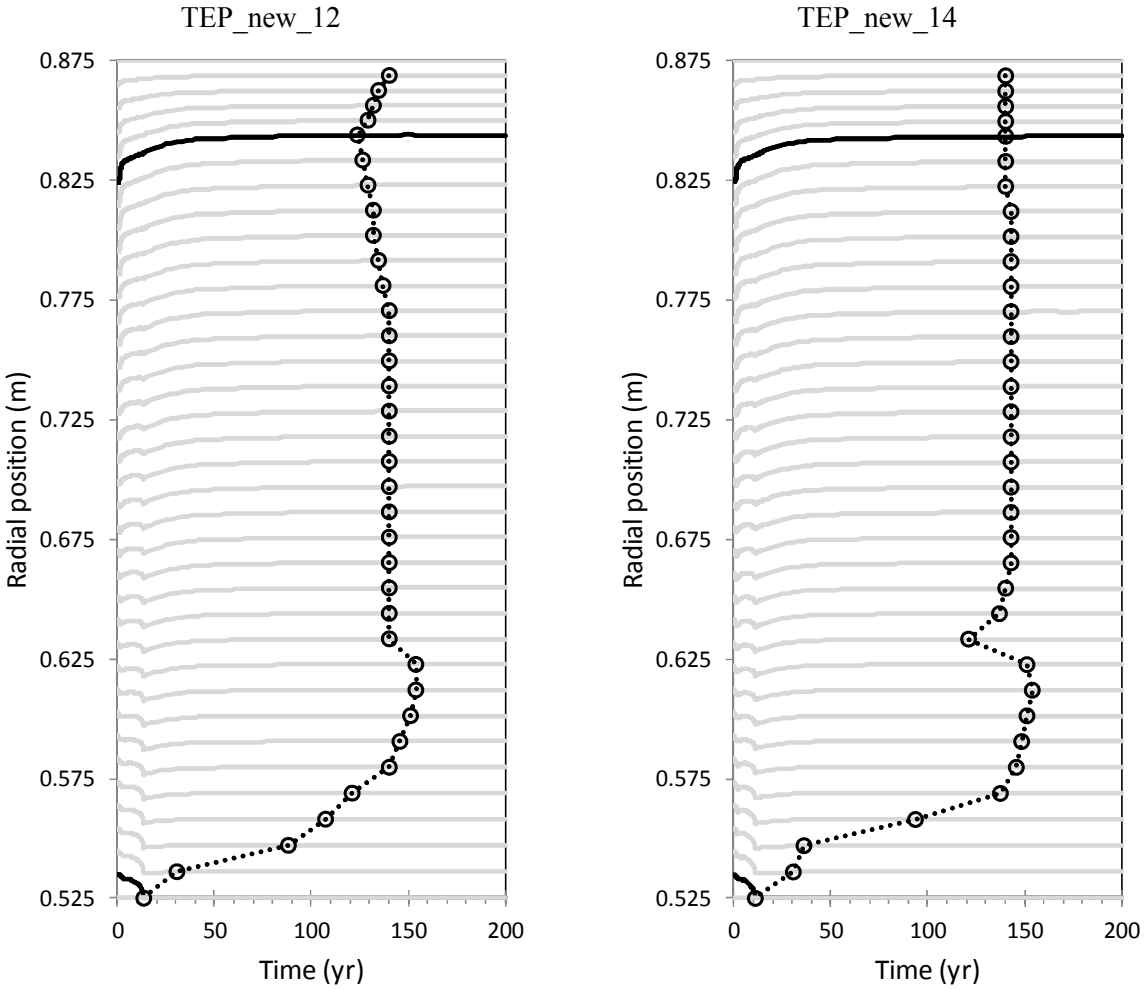

Figure 5. *Local models deformation evolution (solid lines) and isoline consisting of (time, position)-pairs for which the deformation is 0.99 of the final is indicated (hatched),i.e.* $t(|u_r|) \approx 0.99 \cdot |u_r(t=200)|$.

To visualize when and where Buff1 and Buff2 are fulfilled in the models, Figure 6 shows isolines with elements (time, initial radial position) for which $p \approx 1$ MPa (solid) and $p \approx 2$ MPa (hatched). Solution data regarding this analysis are also given in Table 3.

The most conspicuous feature of both isolines is the distinct difference for block and pellet slot. The pellet slot material reach the pressure levels significantly later as compared to neighboring points in the block material. If this is in accordance with reality or just a manifestation of the adopted material representation is, however, not known. Another obvious general feature is the evolution of attaining the pressure levels, first occurring in the outer part of the block material and then progressing inwards. As can be seen, there is some divergence from this trend for $p \approx 1$ MPa in the inner part of the block material close to the initially open inner slot.

It is again stressed that the behavior described above concerns models, and that it is unknown to what degree this agrees with what occur in reality.

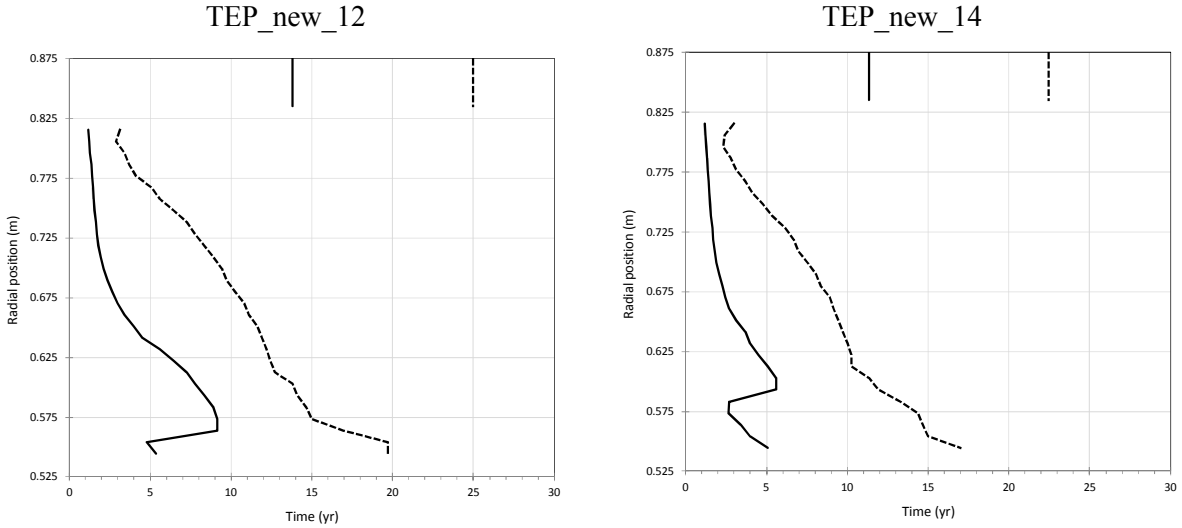

Figure 6. *Local model isolines consisting of (t,r_0)-pairs for which $p \approx 1$ MPa (solid) and $p \approx 2$ MPa (hatched).*

Finally, in order to develop new Buff1 and Buff2 criteria expressed in terms of degree of liquid saturation, the relation of this variable to pressure has to be established. To facilitate this, a procedure similar to what was done when producing the graphs in Figure 6 is utilized. This is based on visualization of when and where Buff1 and Buff2 are fulfilled in the models, again using isolines for which $p \approx 1$ MPa and $p \approx 2$ MPa, but this time the isolines consist of (degree of liquid saturation, initial radial position)-pairs, see Figure 7. In the graphs the initial state of the block and pellet slot material is also indicated for reference. Solution data regarding this analysis are given in Table 3.

Again, as also was the case when studying the graphs in Figure 6, the block and pellet slot materials show distinct differences. In Figure 7 the pellet slot material attains the criteria at a considerable lower degree of saturation as compared to the block material and the isolines also span over a large range which indicate that S_l is not an ideal indicator for pressure in these systems. The lower pressure isoline of the block material has a peculiar feature in the inner part. The lower pressure level (1 MPa) is actually obtained for S_l equal to the initial value S_l^0. Most likely, this comes from the character of the homogenization process where the dry and stiff inner part of the block is compressed by swelling of outer parts and therefore the pressure increases despite no local water uptake in the inner part. This also indicates that S_l is not an ideal indicator for pressure in these systems.

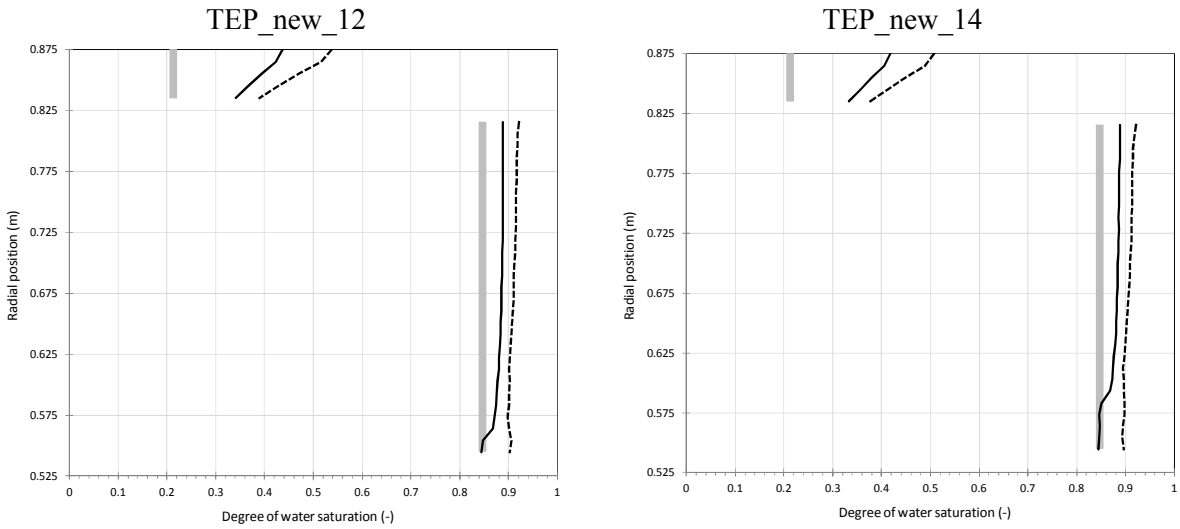

Figure 7. *Local model isolines consisting of (S_l,r_0)-pairs for which $p \approx 1$ MPa (solid black) and $p \approx 2$ MPa (hatched) and initial state (grey).*

Table 3. Solution data for the local models.

Criterion	Model: TEP_new_12		Model: TEP_new_14	
	Block	Pellet slot	Block	Pellet slot
$\|u_r\| \approx 0.99 \cdot \|u_r(t=200)\|$	t = {14, 154} yr	t = {124, 140} yr	t = {11, 154} yr	t = 140 yr
$p \approx 1$ MPa	t = {1.2, 9.2} yr S_l = {0.85, 0.89} VA(S_l)= 0.88	t = 14 yr S_l = {0.34, 0.44} VA(S_l) = 0.39	t = {1.2 , 5.6} yr S_l = {0.85, 0.89} VA(S_l) = 0.88	t = 11 yr S_l = {0.33, 0.42} VA(S_l) = 0.38
$p \approx 2$ MPa	t = {2.9, 20} yr S_l = {0.90, 0.92} VA(S_l) = 0.91	t = 25 yr S_l = {0.39, 0.54} VA(S_l) = 0.47	t = {2.3, 17} yr S_l = {0.89, 0.92} VA(S_l) = 0.91	t = 23 yr S_l = {0.39, 0.54} VA(S_l) = 0.45

5.2 Development of new criteria

First, just to remind the reader, the overall objective is to define intervals in degree of saturation coupled to conditions/events that promote long term safety. The safety functions defined by SKB may be related to criteria expressed in terms of pressure. The task here then is to translate the pressure criteria to criteria given in terms of degree of saturation.

With the former discussion related to the results in Figure 7 in mind, clearly, there exist potential objections for using S_l as a general indicator of pressure. A one-to-one correspondence certainly not exists. In order to reach the objective set out for, a concept of intervals in degree of saturation corresponding to a certain magnitude in pressure will be used.

Since the global and local models do not correspond exactly in terms of initial degree of saturation, S_l^0, relative degree of saturation,

$$S_l^{rel} \equiv \frac{S_l - S_l^0}{1 - S_l^0},$$

will be used when formulating the criteria. In order to obtain criteria manageable when evaluating the global models, they will be formulated in terms of volume averages of relative degree of saturation, $\mathrm{VA}\left({S_l}^{rel}\right)$, over the block material and pellet slot material. During the investigation it was found convenient to work in terms of $\mathrm{VA}(S_l)$, given in Table 3, and ${S_l}^0$ instead of $\mathrm{VA}\left({S_l}^{rel}\right)$ using the relation,

$$\mathrm{VA}\left({S_l}^{rel}\right) = \frac{1}{1-{S_l}^0}\left(\mathrm{VA}(S_l) - {S_l}^0\right).$$

The chosen criteria formulated in terms of a range in $\mathrm{VA}\left({S_l}^{rel}\right)$ defined by minimum and maximum values. These values are obtained from evaluating the ${S_l}^{rel}$-response of the local models. A single criterion is defined by,

$$\begin{aligned} \text{criterion} &\equiv \{\text{minimum}, \text{maximum}\} \\ \text{minimum} &\equiv \mathrm{VA}\left({S_l}^{rel}\right) - \left(\max\left({S_l}^{rel}\right) - \mathrm{VA}\left({S_l}^{rel}\right)\right) \\ \text{maximum} &\equiv \max\left({S_l}^{rel}\right) \end{aligned}$$

When calculating the criteria based on the expressions above, the values given in Table 4 are obtained.

Table 4. First version of new Buff1 and Buff2 criteria expressed in terms of relative degree of liquid saturation for the block and pellet slot materials.

	Criterion expressed in p	Criterion expressed in $\mathrm{VA}(S_l^{rel})$	
		Block	Pellet slot
Buff1	≈ 1 MPa	{0.145, 0.278}	{0.165, 0.285}
Buff2	≈ 2 MPa	{0.302, 0.487}	{0.225, 0.414}

Figure 8 shows the criteria graphically, indicated by the grey solid and grey hatched lines, for Buff1 (solid grey) and Buff2 (hatched grey), respectively. The criteria are shown together with the same information as Figure 7, but now expressed in terms of ${S_l}^{rel}$. As the criteria are designed, they exclude the "tail" of low values of saturation in the block material close to the canister. The criteria are considered on the conservative side in the sense that they most likely overestimate the time until Buff1 and Buff2 are fulfilled.

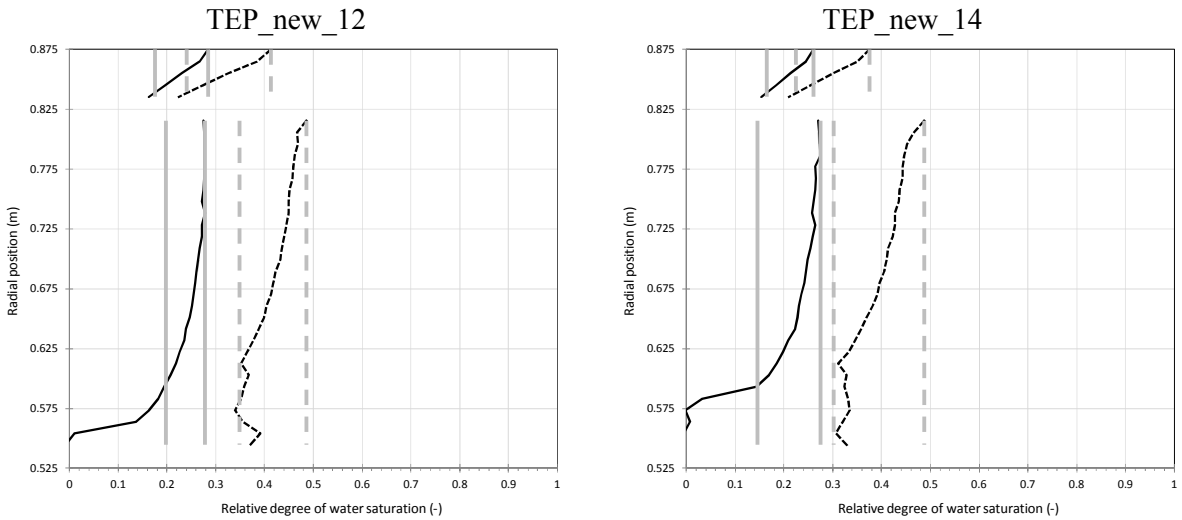

Figure 8. *Local model isolines consisting of (S_l^{rel},r_0)-pairs for which p ≈ 1 MPa (solid black) and p ≈ 2 MPa (hatched black). Also, the adopted minimum and maximum limits are indicated in solid and hatched grey lines, for Buff1 and Buff2, respectively.*

5.3 Evaluation and refinement of new criteria

The first versions of the new criteria, expressed in $\mathrm{VA}(S_l^{rel})$, are here to be evaluated. Time intervals when the new S_l^{rel} criteria are reached in the global models, 2I and 2H, are compared with time intervals when the criteria expressed in *p* are reached in the local models, TEP_new_12 and TEP_new_14. The analysis is performed at canister mid-height of the global models in order to obtain as clear comparison to the local models as possible.

In Figure 9 the global model response in terms of volume averages of relative degree of liquid saturation formed over the block and pellet slot at canister mid-height, as well as the first version criteria as listed in Table 4 are shown. As for the pellet slot it was discretized using two elements radially, thus three nodes where two belong to interfaces and the mid node belong to the pellet slot material solely. The volume average is therefore taken as the result at the mid-node. The time intervals obtained from applying the criteria in Table 4 on the evolution curves in Figure 9 are listed in Table 5.

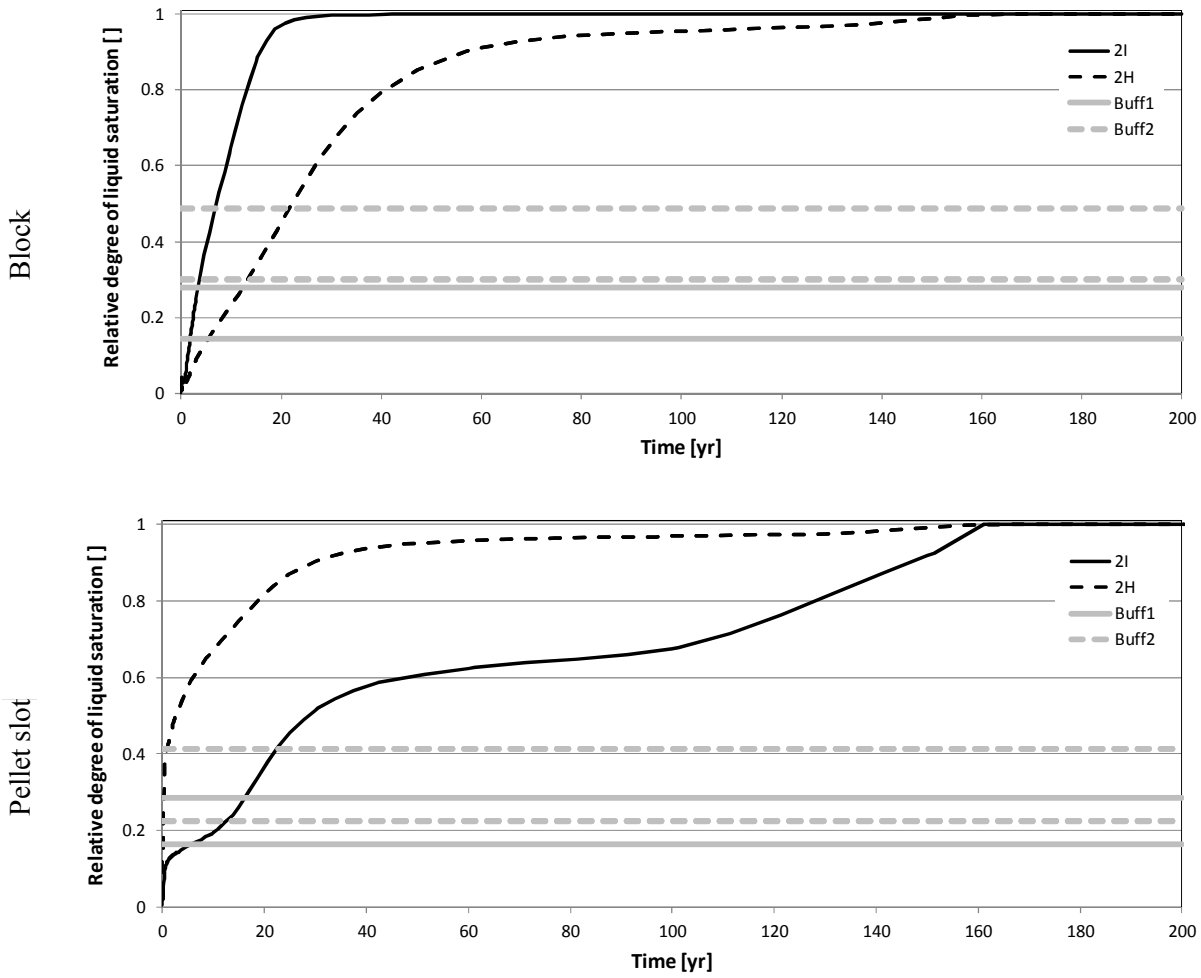

***Figure 9**. Evolution of volume averages of relative degree of liquid saturation, $VA(S_l^{rel})$ for global models 2I and 2H are shown together with the first version of S_l criteria. The volume averages over the pellet slot and buffer are formed at canister mid-height.*

Table 5. Obtained times (in years) when the adopted S_l criteria are fulfilled for global models 2I and 2H.

	Model: 2I		Model: 2H	
	Block	Pellet slot	Block	Pellet slot
Buff1	t={1.8, 3.4}	t={5.8, 16}	t={5.5, 12}	t={0.058, 0.22}
Buff2	t={3.7, 6.8}	t={13, 23}	t={13, 22}	t={0.26, 2.3}

Plotting the time intervals when the p and S_l criteria are reached in the block and pellet slot materials for the local models (in grey) and global models (thin black lines), gives the diagrams shown in Figure 10. In addition, the thick black lines indicate combined considerations of both global models, i.e. overall maximum and minimum values for both global models.

For the block material, the global models together with the first version criteria produces time intervals for Buff1 and Buff2, which are in good agreement with those of the local models. Therefore, no adjustments are made to the first version criteria for the block material.

For the pellet slot material, the global models together with the first version criteria do not match the results of the local models well for either Buff1 or Buff2. For Buff1 the homogenized global model (2H) severely underestimates the time until Buff1 is reached, whereas the time interval of the initial state model (2I) includes the local time interval. For Buff2, however, the time until fulfilment is significantly underestimated by 2H and somewhat underestimated by 2I. An adjusted criterion is therefore regarded necessary for the pellet slot material.

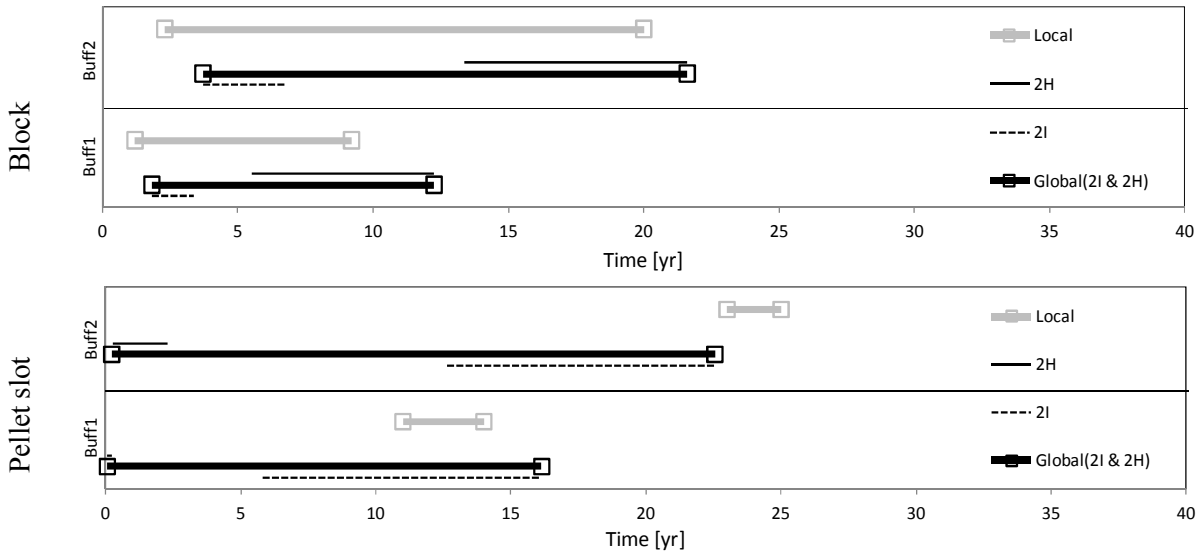

Figure 10. *Time intervals when the first version criteria are reached for the local models (grey) and global models, 2I (thin black solid) and 2H (thin black hatched). The thick black solid lines indicate the time intervals resulting from using the combined result of both global models. Note that the criteria generating the above are expressed in pressure for the local (THM) models and in degree of liquid saturation for the global (TH) models.*

To get better correspondence between the global and local time intervals for the pellet slot material without complicating things too much, the maximal criterion of Buff2 is chosen equal to that of the block material ($\mathrm{VA}(S_l^{rel}) > 0.487$) and only the initial state model (2I) is considered in the "combined" consideration.

The result from these adjustments can be seen when studying Figure 11 and the final version of the criteria, used in the evaluation, is shown in Table 6.

The adjustments described above might seem rough, but it should be remembered that the homogenized global model has a very oversimplified representation of the pellet slot material and by disregarding this one may say that a higher degree of accuracy has been obtained. Also, when using the adjusted criteria, the global time intervals include the corresponding local time intervals and obtain lower limits closer to the local model intervals.

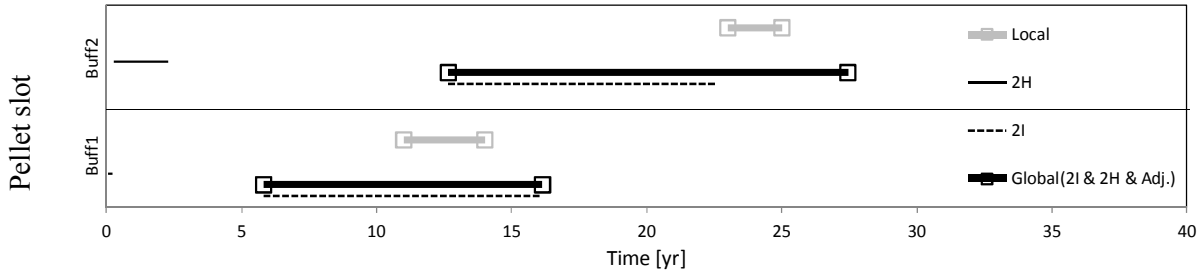

Figure 11. *Time intervals when the adjusted pellet slot criteria limits are reached for the local models (grey) and global models, 2I (thin black solid) and 2H (thin black hatched). The thick black solid lines indicate the time intervals resulting from using the adjusted pelllet slot criteria where only the time interval of 2I is considered. Note that the criteria generating the above are expressed in pressure for the local (THM) models and in degree of liquid saturation for the global (TH) models.*

Table 6. Final version of adjusted Buff1 and Buff2 criteria expressed in terms of relative degree of liquid saturation for the block and pellet slot materials.

	Criterion expressed in *p*	Criterion expressed in VA(S_l^{rel})	
		Block	Pellet slot*
Buff1	≈ 1 MPa	{0.145, 0.278}	{0.165, 0.285}
Buff2	≈ 2 MPa	{0.302, 0.487}	{0.225, 0.487}

* Only the results of the initial state model are to be considered for the pellet slot material.

6 Investigation of fulfilment of Buff1 and Buff2 in global TH models

The fulfilment of the criteria is studied at a number of positions in the DH-buffer as shown in Figure 12. There are five positions at different heights: below canister, mid canister, above canister, top of buffer, and top of deposition hole, and three "radial positions" (or rather cross-sectional areas): inner block (IB), outer block (OB), and pellet slot (P), for which the criteria are evaluated. It is assumed that due to the geometric and structural similarity at different heights, the criteria found relevant at canister mid-height, shown in Table 6, also can be used to obtain reasonable estimations at other positions as well. Moreover, the influence of the open slot, not present in the buffer below and above the canister, was suppressed when designing the new criteria. This should bring the state for which the criteria were designed "closer to" what the cylinder-shaped blocks "experience".

Two different cases have been considered, first, the case with a hydraulic conductivity of the rock equal to $K_R = 10^{-12}$ m/s, represented by models 2I and 2H, and secondly, a case with a hydraulic conductivity of the rock equal to $K_R = 10^{-13}$ m/s, represented by models 8I and 8H. Since the criteria were developed using a 1-D model which was calibrated to represent a slow wetting process, it is here assumed that the criteria, verified for $K_R = 10^{-12}$ m/s, are valid for systems using the lower hydraulic conductivity, $K_R = 10^{-13}$ m/s, as well.

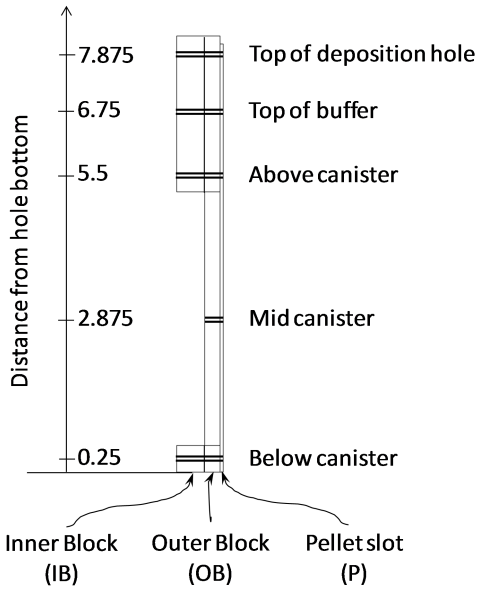

Figure 12. *Positions and notation regarding where the criteria are evaluated for the global models.*

For the case where $K_R = 10^{-12}$ m/s (model 2I and 2H), the results are given in graphical and tabulated form in Figure 13 and Figure 14 for Buff1 and Buff2, respectively. The shaded regions with different outlines (solid, hatched, and dot-hatched) for the different buffer volumes as defined in Figure 12 (IB, OB, and P, respectively) represent what will be called "criteria fulfilment surface" (CFS).

As clearly seen in Figure 13 and Figure 14 when studying the appearance of the pellet slot CFS, there is a general trend, for both Buff1 and Buff2, in that the criteria are fulfilled "from the bottom to the top" in the pellet slot. The time intervals of the pellet slot are also generally later in time when

comparing with the other material volumes at the same height, the only exception being at the bottom for Buff1.

Another common feature for Buff1 and Buff2 is the shift to the right of the inner block CFSs' (thus, its later occurrence in time) as compared to the outer block's, with the exception at the top position for both Buff1 and Buff2. The overall shape of the CFSs is also similar between Buff1 and Buff2. A distinct kink in the inner block's CFS, delaying the fulfilment, is present in the position above the canister for Buff1 and Buff2. On the other hand, at the same position, the outer block CFSs are shifted towards an earlier fulfilment.

If trying to elaborate on the reason behind the CFS shape at the canister top, it could be said that the material in the inner block volume on top of the canister will generally be relatively dry due to the proximity to the heat source and distance to the water bearing rock. The water will be transported outwards in form of vapour that counteracts the inward liquid water transport from the rock. Therefore, the water uptake in the inner block material will be restrained and the material in the outer block may have an influx of water in terms of vapour which will enhance the water uptake.

As also can be seen, the criteria fulfilment occurs late at the top of the deposition hole. This comes from the proximity to the tunnel backfill, "competing" with the buffer about the water.

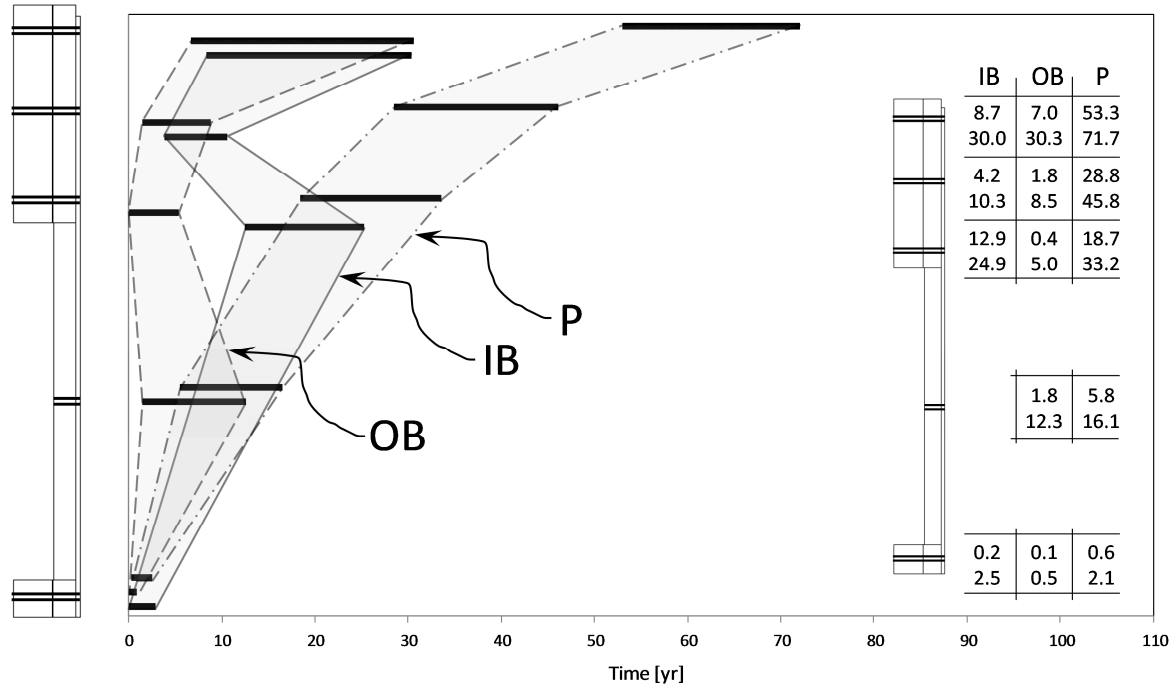

Figure 13. *Compilation of estimated time intervals for which safety function Buff1 are reached at the indicated positions for models with rock conductivity 10^{-12} m/s and no fractures, i.e. 2I and 2H in (Åkesson et al. 2010, chapter 3). In the table to the right the start (top) and end (bottom) of the time interval are given for each of the positions.*

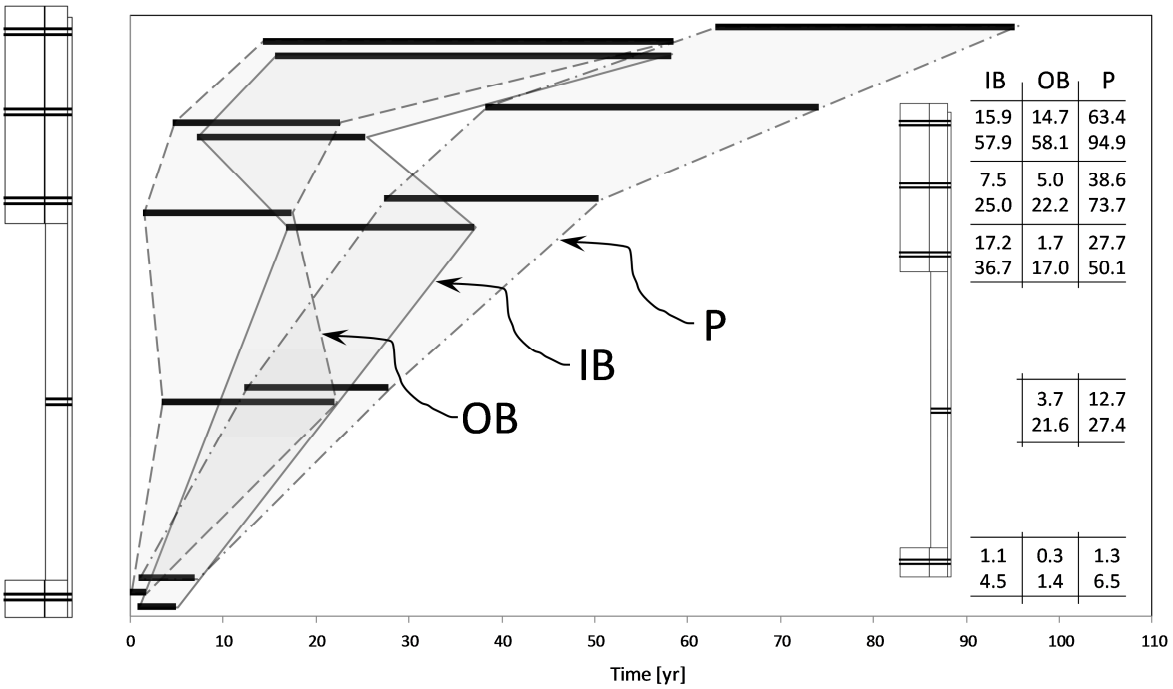

Figure 14. *Compilation of estimated time intervals for which safety function Buff2 are reached at the indicated positions for models with rock conductivity 10^{-12} m/s and no fractures, i.e. 2I and 2H in (Åkesson et al. 2010, chapter 3). In the table to the right the start (top) and end (bottom) of the time interval are given for each of the positions.*

If considering the case where $K_R = 10^{-13}$ m/s (model 8I and 8H) the results given in Figure 15 and Figure 16 for Buff1 and Buff2, respectively, are obtained. As can be seen, the CSFs have a lot in common with those of the case where $K_R = 10^{-12}$ m/s:

- For the pellet slot the criteria are fulfilled late in time and from the bottom to the top.
- The inner block CFS is to the right (later in time) as compared to the outer block CFS.
- A rightward kink (a "delay") of the inner block CFS can be seen above the canister.

There are, however, some special features for the $K_R = 10^{-13}$ m/s case as well. The position of the pellet slot CFS is further to the right (later in time) as compared to the block volumes and the shape is also somewhat different from what is seen for $K_R = 10^{-12}$ m/s. It could also be mentioned that the Buff1 criterion giving the end point of the pellet slot interval below the canister (225.2 yr) was crossed the first time at 11.2 yr, but a subsequent drying of the material made the saturation level go down below the criterion again. The same happened in the pellet slot at the same position but for the Buff2 criterion which gives the start point of the interval (144.9 yr), the time at the first fulfilment of the criterion was 5.9 yr.

Finally, in Figure 17, all results are compiled for facilitating comparisons between the $K_R = 10^{-12}$ m/s and $K_R = 10^{-13}$ m/s case.

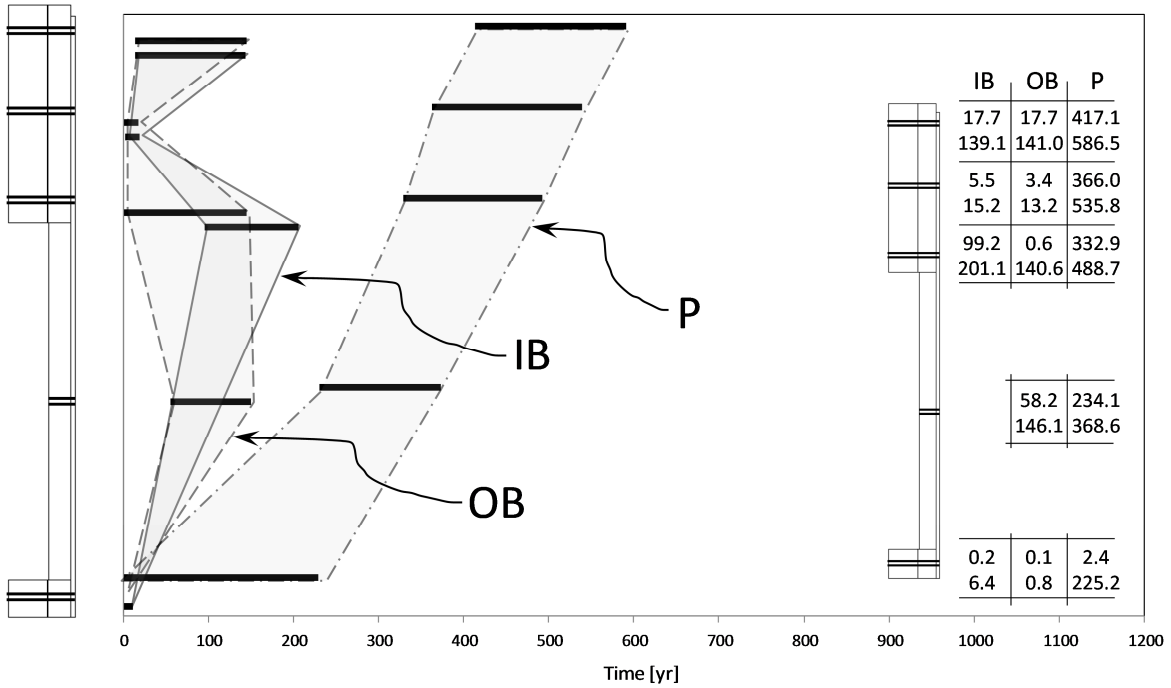

Figure 15. *Compilation of estimated time intervals for which safety function Buff1 are reached at the indicated positions for models with rock conductivity 10^{-13} m/s and no fractures, i.e. 8I and 8H in (Åkesson et al. 2010, chapter 3). In the table to the right the start (top) and end (bottom) of the time interval are given for each of the positions.*

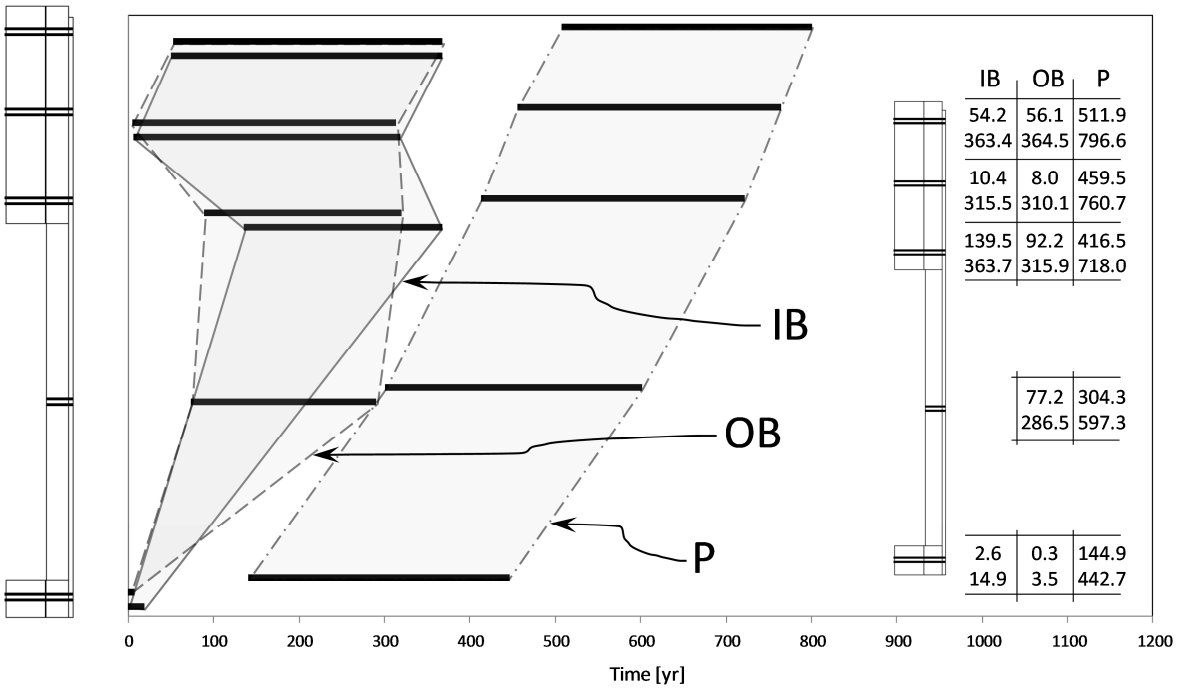

Figure 16. *Compilation of estimated time intervals for which safety function Buff2 are reached at the indicated positions for models with rock conductivity 10^{-13} m/s and no fractures, i.e. 8I and 8H in (Åkesson et al. 2010, chapter 3). In the table to the right the start (top) and end (bottom) of the time interval are given for each of the positions.*

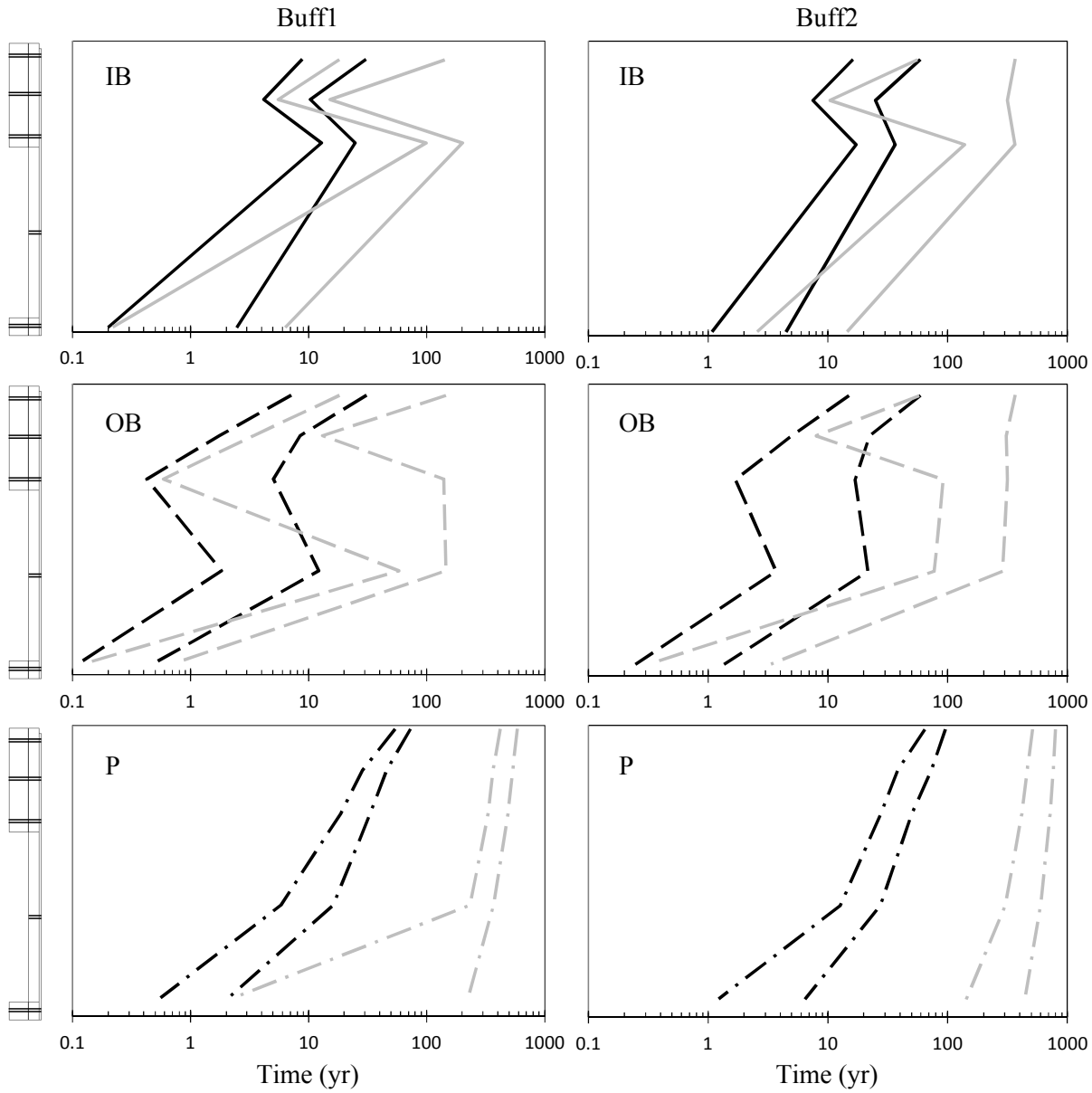

Figure 17. *Compilation of estimated time intervals (given by the horizontal distance between similar lines) for which safety functions Buff1 (left column) and Buff2 (right column) are reached in different buffer volumes (Inner Block=IB, Outer Block=OB, and Pellet slot=P) at different height from the deposition hole bottom. Results are shown for cases with rock conductivity 10^{-12} m/s (black lines) or 10^{-13} m/s (grey lines) and no fractures, i.e. (2I, 2H) and (8I, 8H) in (Åkesson et al. 2010, chapter 3), respectively.*

7 Summary and conclusions

Here, an attempt to meet SSM's request of an analysis where intervals in the saturation process are coupled to long time safety (SSM2011-2426-81) is carried out. SSM suggested that intervals in degree of saturation should be coupled to conditions/events that promote long term safety such as: build up of pressure to reduce microbial activity, and closure of open gaps close to the canister and deposition hole (DH) wall.

These conditions/events that promote long time safety are related to the so called safety functions, their safety function indicators, and corresponding safety function indicator criteria for the buffer as described in the SR-Site main report (SKB 2011). Criteria considered relevant for this study, related to "Limiting advective transport" and "Reduce microbial activity", were expressed in terms of pressure.

Local 1D axisymmetrical THM simulations were performed and utilized to translate the criteria, expressed in pressure, into new criteria expressed in intervals of degree of saturation, as requested by SSM, see Table 6 repeated below.

Table 6 repeated: Final version of adjusted Buff1 and Buff2 criteria expressed in terms of relative degree of liquid saturation for the block and pellet slot materials.

	Criterion expressed in p	Criterion expressed in VA(S_l^{rel})	
		Block	Pellet slot*
Buff1	≈ 1 MPa	{0.145, 0.278}	{0.165, 0.285}
Buff2	≈ 2 MPa	{0.302, 0.487}	{0.225, 0.487}

* Only the results of the initial state model are to be considered for the pellet slot material.

These criteria, given in terms of intervals of volume averages of relative degree of saturation, were then applied on two sets of TH-models, described in (Åkesson et al. 2010, chapter 3), and the safety functions' fulfillment process in a DH-buffer was then studied, see Figure 13 - Figure 17.

Below follows a list of conclusions from the investigation:

- The current safety functions given by SKB are only defined for fully water saturated conditions. The present study disregards this and only considers the safety function criteria expressed in pressure without taking into account the level of saturation.
- The used mechanical material representation is process dependent and has to be calibrated for different situations. Here a slow wetting process was considered and mechanical parameters of the pellet slot had to be chosen as to generate a representative density profile at full water saturation.
- Processes in the buffer are heterogeneous. The models show large differences between the block and pellet slot materials as well as within the block and pellet slot materials.
- Degree of water saturation is not found to be an ideal indicator for pressure in the buffer system. The buffer attains a specified pressure for quite a large range of degree of water

saturation, absolute or relative. That is why the criteria in Table 6 are given in terms of intervals.

- Safety function criteria are fulfilled heterogeneously within the buffer. The general trend is "from the bottom to the top" and "later in the pellet slot".
- For the cases investigated, the hydraulic conductivity of the rock material is a crucial characteristic of the system, which significantly affects the time until fulfillment of the safety functions.
- The general "relative" trend of the safety function fulfillment process for the two different rock hydraulic conductivities studied has strong similarities.

8 References

SKB, 2006. Buffer and backfill process report for the safety assessment SR-Can. SKB TR-06-18, Svensk Kärnbränslehantering AB.

SKB, 2011. Long-term safety for the final repository for spent nuclear fuel at Forsmark. Main report of the SR-Site project. SKB TR-11-01, Svensk Kärnbränslehantering AB

Åkesson M, Kristensson O, Börgesson L, Dueck A, Hernelind J, 2010. THM modeling of buffer, backfill and other system components. Critical processes and scenarios. SKB TR-10-11, Svensk Kärnbränslehantering AB.

Appendix A Mesh dependence investigation

When increasing the number of elements in the radial direction by a factor of three in the block and pellet slot, no significant change could be seen in the responses. This indicates that the coarser discretization is fine enough for the used element type.

Table A1-1. Models used in the mesh dependence study.

Model name	No. of elements radially		
	Open slot	Block	Pellet slot
TEP_new_12	1	30	5
TEP_new_12_fine	1	90	15

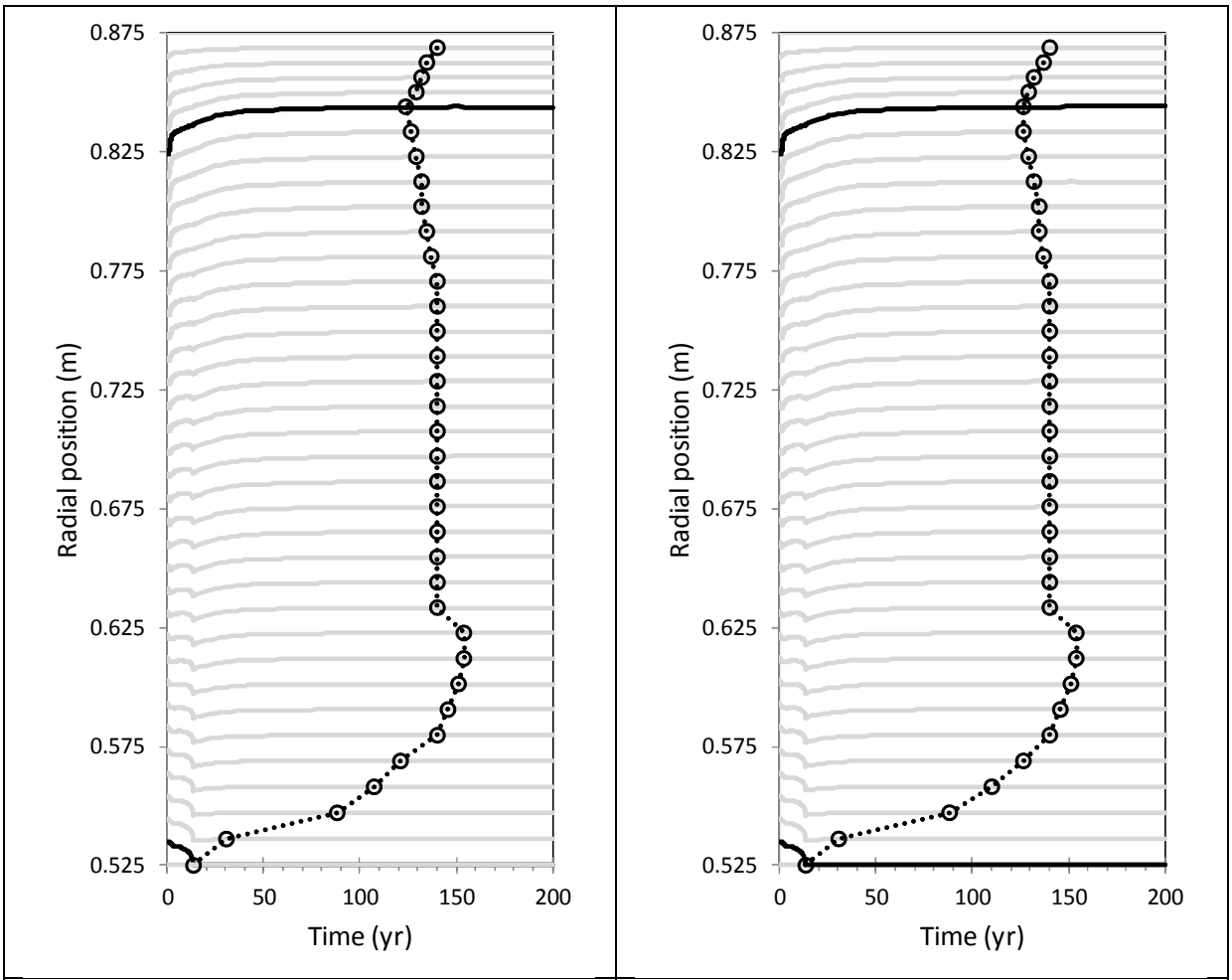

Figure A1-1. *Local models deformation evolution (solid lines) and isoline consisting of pairs (time, position) for which the deformation is 0.99 of the final is indicated (hatched),i.e.* $t(|u_r|) \approx 0.99 \cdot |u_r(t=200)|$.

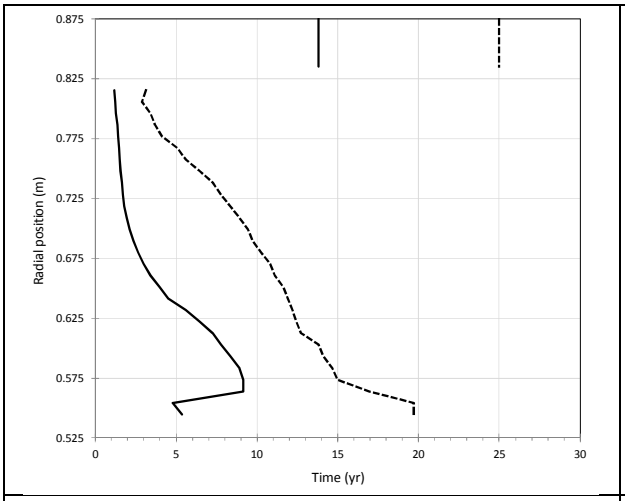

TEP_new_12

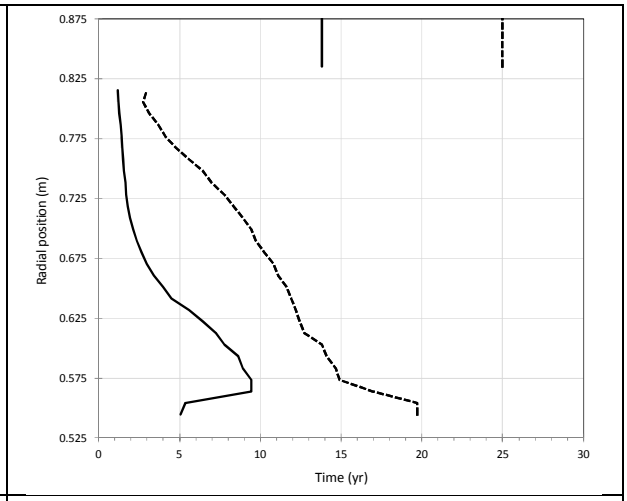

TEP_new_12_fine

Figure A1-2. *Local model isolines consisting of pairs* (t,r_0) *for which p ≈ 1 MPa (solid) and p ≈ 2 MPa (hatched).*

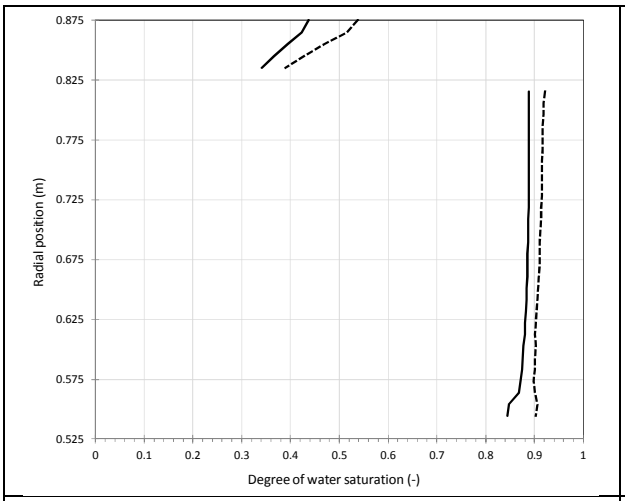

TEP_new_12

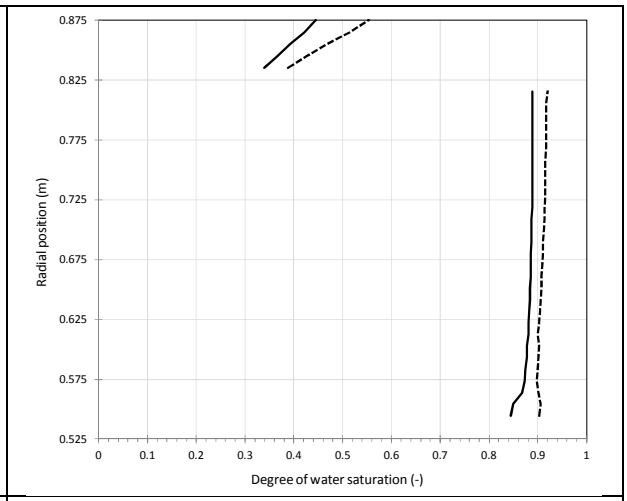

TEP_new_12_fine

Figure A1-3. *Local model isolines consisting of pairs* (S_l,r_0) *for which p ≈ 1 MPa (solid) and p ≈ 2 MPa (hatched).*

Appendix B Model catalogue

Location: ”Administrativa dokument on”:\ Projekt\ SR-Site SSM-frågor\data\modeller\ Task_3.1*

Table A2-1. Local models used in this study.

Model name	GiD-directory
TEP_new_12	TEP_new_12.gid
TEP_new_14	TEP_new_14.gid
TEP_new_12_fine	TEP_new_12_fine.gid

Table A2-2. Global models used in this study.

Model name	GiD-dir.
2I	THsat13.gid
2H	THsat14.gid
8I	THsat20I2.gid
8H	THsat20H4.gid